Physics and Imaging in Radiation Oncology 27 (2023) 100466

Contents lists available at ScienceDirect

Physics and Imaging in Radiation Oncology

journal homepage: www.sciencedirect.com/journal/physics-and-imaging-in-radiation-oncology

Original Research Article

Linear energy transfer-inclusive models of brainstem necrosis following proton therapy of paediatric ependymoma

Andreas H. Handeland [a,b,*], Daniel J. Indelicato [c], Lars Fredrik Fjæra [a,d], Kristian S. Ytre-Hauge [a], Helge Egil S. Pettersen [b], Ludvig P. Muren [e,f], Yasmin Lassen-Ramshad [e], Camilla H. Stokkevåg [a,b]

[a] Department of Physics and Technology, University of Bergen, Bergen, Norway
[b] Department of Oncology and Medical Physics, Haukeland University Hospital, Bergen, Norway
[c] Department of Radiation Oncology, University of Florida, Jacksonville, FL, USA
[d] Department of Medical Physics, Oslo University Hospital, Norway
[e] Danish Centre for Particle Therapy, Aarhus University Hospital, Aarhus, Denmark
[f] Department of Clinical Medicine, Aarhus University, Aarhus, Denmark

ARTICLE INFO

Keywords:
Proton therapy
Pediatric
Relative biological effectiveness
Normal tissue complication probability
Brainstem necrosis
Ependymoma
Linear energy transfer

ABSTRACT

Background and Purpose: Radiation-induced brainstem necrosis after proton therapy is a severe toxicity with potential association to uncertainties in the proton relative biological effectiveness (RBE). A constant RBE of 1.1 is assumed clinically, but the RBE is known to vary with linear energy transfer (LET). LET-inclusive predictive models of toxicity may therefore be beneficial during proton treatment planning. Hence, we aimed to construct models describing the association between brainstem necrosis and LET in the brainstem.

Materials and methods: A matched case-control cohort (n = 28, 1:3 case-control ratio) of symptomatic brainstem necrosis was selected from 954 paediatric ependymoma brain tumour patients treated with passively scattered proton therapy. Dose-averaged LET (LET_d) parameters in restricted volumes ($L_{50\%}$, $L_{10\%}$ and $L^{3}_{0.1cm}$, the cumulative LET_d) within high-dose thresholds were included in linear- and logistic regression normal tissue complication probability (NTCP) models.

Results: A 1 keV/μm increase in $L_{10\%}$ to the brainstem volume receiving dose over 54 Gy(RBE) led to an increased brainstem necrosis risk [95% confidence interval] of 2.5 [0.0, 7.8] percentage points. The corresponding logistic regression model had area under the receiver operating characteristic curve (AUC) of 0.76, increasing to 0.84 with the anterior pons substructure as a second parameter. 19 [7, 350] patients with toxicity were required to associate the $L_{10\%}$ ($D > 54$ Gy(RBE)) and brainstem necrosis with 80% statistical power.

Conclusion: The established models of brainstem necrosis illustrate a potential impact of high LET regions in patients receiving high doses to the brainstem, and thereby support LET mitigation during clinical treatment planning.

1. Introduction

Ependymomas are paediatric intra-cranial brain tumours forming through the ependymal cells lining passageways of cerebrospinal fluid [1]. Radiotherapy is an important part of treating ependymoma and is commonly administered following surgical removal of the solid tumour [1,2]. Proton therapy is increasingly used in these patients due to tissue sparing capabilities compared to conventional radiotherapy, and with an expected lower risk of toxicity [2].

Radiation-induced brainstem necrosis is a severe toxicity attributed to dose exposure of the brainstem during radiotherapy of ependymoma [2,3]. Children are generally more radiosensitive compared to adults, which means that established tolerance doses from adult patients are not directly applicable in paediatric patients [4]. Furthermore, proton radiation is more effective at cell-killing compared to photons [5], which is accounted for clinically by multiplying the physical proton dose with a relative biological effectiveness (RBE) factor of 1.1. However, it is well known that the proton RBE is spatially variable depending on the linear energy transfer (LET), the $(\alpha/\beta)_x$ of the tissue, as well as total dose and applied fractionation [6]. Clinical evidence of a variable RBE is,

* Corresponding author at: Department of Oncology and Medical Physics, Haukeland University Hospital, Bergen, Norway.
E-mail addresses: andreas.havsgard.handeland@helse-bergen.no, andreas.handeland@uib.no (A.H. Handeland).

https://doi.org/10.1016/j.phro.2023.100466
Received 17 February 2023; Received in revised form 22 June 2023; Accepted 24 June 2023
Available online 29 June 2023

however, inconclusive [7,8]. Several studies have observed associations between high LET and localised development of symptomatic brain toxicity or MR image changes [9–18]. Most investigations are retrospective and uncontrolled, with relatively small data sets [7]. In a previous study we utilised a matched case-control design and found trends in increasing LET with incidence of paediatric brainstem necrosis [19].

Photon-based normal tissue complication probability (NTCP) models disregard potential RBE effects such as LET differences and may consequentially have inferior performance when applied in proton therapy cohorts [20,21]. Developing NTCP models specific to proton radiotherapy could therefore be an important step in advancing clinical integration of LET [21]. Furthermore, a matched retrospective case-control design could reduce effects of confounding factors and may be better suited for identification of variable RBE effects in a limited cohort size [22]. In this study we developed LET-inclusive NTCP models for symptomatic brainstem necrosis based on a paediatric ependymoma

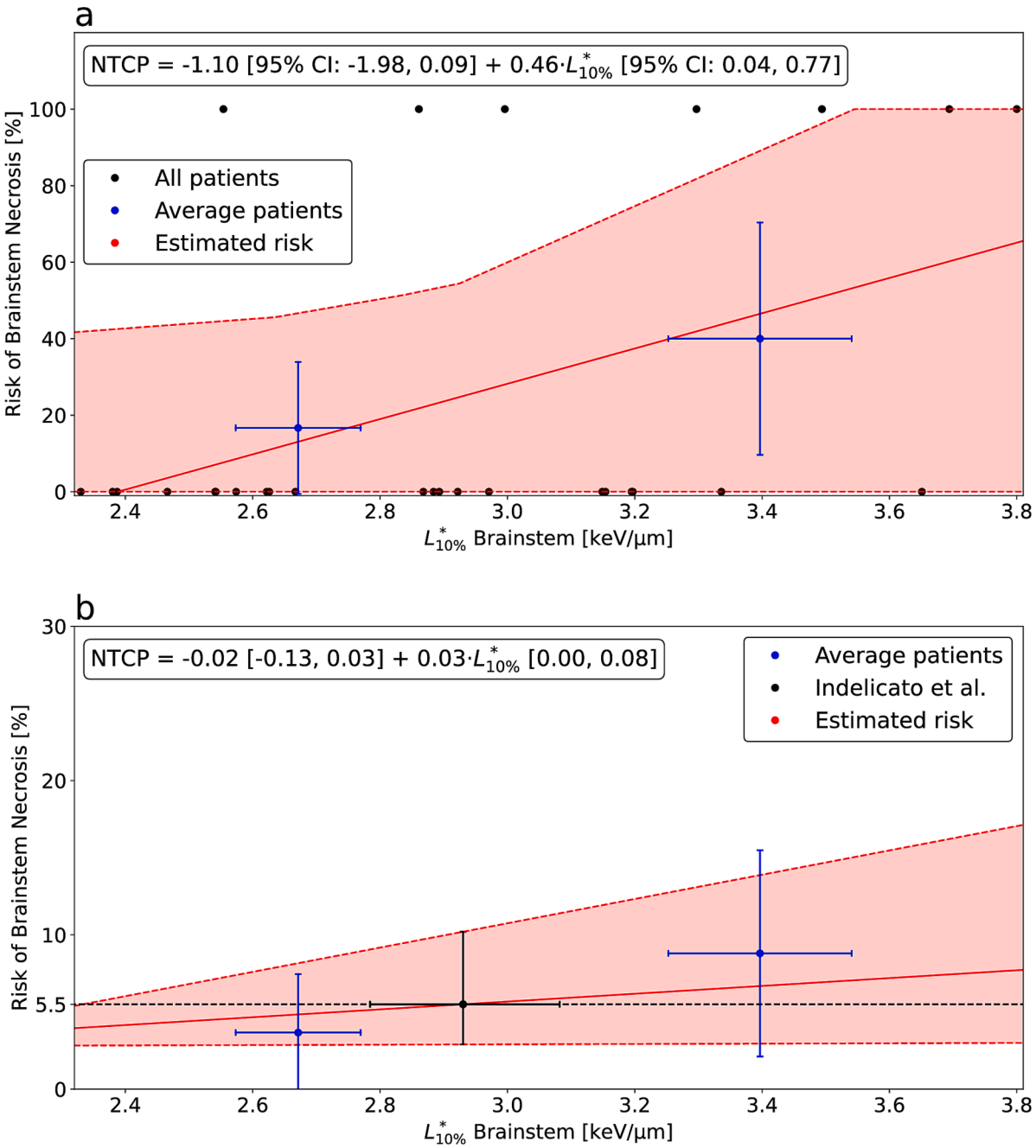

Fig. 1. Univariate linear regression models of brainstem necrosis risk as a function of the LET_d to the 10% of the full brainstem volume ($L_{10\%}$) receiving an RBE-weighted dose over 54 Gy(RBE) with $RBE_{1.1}$ marked with a *. 95% CIs for the regression curves are shown in dashed red lines with the shaded red area describing the area covered by the CIs. a) shows a linear regression model describing relative risk associated with the $L_{10\%}$ ($D > 54$ Gy(RBE)) based on only the cohort in this work. Each individual patient in the case-control cohort is plotted as a black point. The case-control cohort is also shown divided into two groups with the average $L_{10\%}$ ($D > 54$ Gy(RBE)) of all patients either over or under 3 keV/µm plotted in blue with 95% CIs in both average $L_{10\%}$ ($D > 54$ Gy(RBE)) and toxicity incidence plotted along their respective axes. b) is a linear regression model showing absolute risk of brainstem necrosis also associated with the $L_{10\%}$ ($D > 54$ Gy (RBE). The incidence rate is scaled to an incidence rate of 5.5% [95% CI: 2.9%, 10.2%] [25] at an $L_{10\%}$ ($D > 54$ Gy(RBE)) of 2.93 keV/µm [95% CI: 2.78, 3.08]) (shown in black). The case-control cohort shown in blue is also scaled down with the same scaling factor that was used to achieve the incidence rate. (For interpretation of the references to colour in this figure legend, the reader is referred to the web version of this article.)

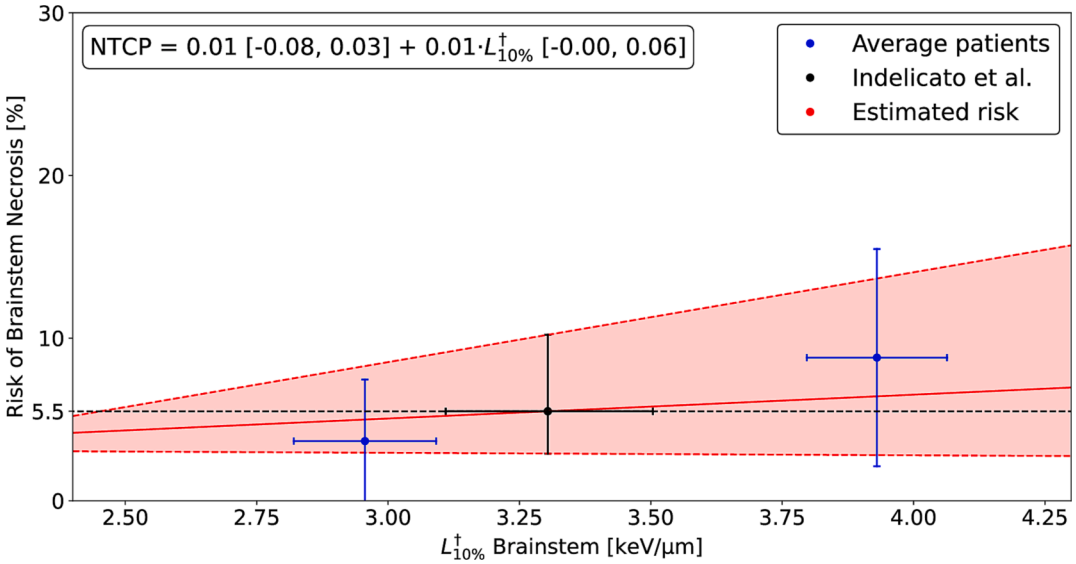

Fig. 2. Linear regression model showing absolute risk of brainstem necrosis associated with the $L_{10\%}$ ($D > 50$ Gy(RBE) marked with a †. 95% CIs for the regression curves are shown in dashed red lines with the shaded red area describing the area covered by the CIs. The incidence rate is scaled to an incidence rate of 5.5% [95% CI: 2.9%, 10.2%] [25] at an $L_{10\%}$ ($D > 54$ Gy(RBE)) of 2.93 keV/μm [95% CI: 2.78, 3.08]) (shown in black). The case-control cohort is divided based on whether the patients have $L_{10\%}$ ($D > 50$ Gy(RBE) over or under 3.5 keV/μm and are shown in blue scaled down with the same scaling factor that was used to achieve the incidence rate. (For interpretation of the references to colour in this figure legend, the reader is referred to the web version of this article.)

cohort treated with proton therapy. The applied study design and included parameters were also used to estimate the expected number of ependymoma patients required to establish robust LET-inclusive RBE models of brainstem toxicity.

2. Materials and methods

2.1. Patient selection and dose calculation

From a total cohort of 954 paediatric patients treated with passively scattered proton therapy for brain tumours at the University of Florida Health Proton Therapy Institute (UFHPTI) between 2006 and 2017, 28 paediatric ependymoma brain tumour patients were selected for this analysis in a matched case-control design (1:3 case-control ratio). More details on patient selection are included in Supplementary material A [19].

All included DICOM and patient data were part of an institutional review board-approved study and were anonymised prior to export of dosimetric data and analysis. Dose and dose-averaged LET (LET_d) distributions were calculated with the FLUKA Monte Carlo code with all nozzle components from the original treatment implemented [23]. The radiation was simulated in the patient CTs and both dose and LET_d were scored in water, with the former considering all particles, while the latter considered primary and secondary protons only.

2.2. Statistical analysis

Parameters included for analysis were LET_d and $RBE_{1.1}$-weighted doses to volume segments 50%, 10% and 1 cm^3 (denoted $L_{50\%}$, $L_{10\%}$ and $L^3_{0.1cm}$ for LET_d, respectively), as well as the volume of the full brainstem. The LET_d parameters considered the brainstem voxels receiving doses over specified dose thresholds with cumulative LET_d representing the specified fraction of the voxels with the highest LET_d values. Several dose thresholds were explored but 1 Gy(RBE), 50 Gy(RBE) and 54 Gy (RBE) were selected for the final analysis and presented in this work. The 1 Gy(RBE) parameter was used to exclude very low dose voxels only, while 50 and 54 Gy(RBE) exclude all but the highest dose voxels instead. The statistical analysis is further described in Supplementary material B.

2.3. Parameter selection

Parameters were selected for the models based on bootstrapping in 10^4 iterations. Univariate models with each parameter (Fig. A2 and A3) were trained using the bootstrapped samples. The parameter was then removed and the change in Akaike information criterion (AIC) and Schwarz' Bayesian information criterion (BIC) was assessed. The resulting model was chosen based on the greatest improvement in AIC and BIC between having one and no parameters, thus a model with intercept only. The same procedure was followed for the second parameter of the bivariate model. The 50 Gy(RBE) dose threshold was excluded from the parameter selection.

2.4. Predictive modelling

We chose to primarily focus on a linear regression model, rather than a more standard NTCP-model such as logistic regression, due to the lack of incidence data in this case-control cohort and the overall low incidence of brainstem necrosis after proton therapy. The linear function can be considered an approximation of the linear behaviour of the sigmoid curve at low risk levels. We fit the risk to a curve $B_s(1+kx)$ similarly to the methods described by Darby et al. to model the risk of ischemic heart disease following radiotherapy of breast cancer [24]. Here B_s is a base rate, while k is the linear percentage increase in risk per parameter unit, and $\times$ is the modelled parameter. The base rate, B_s, was not a y-axis intercept in our case but rather an intercept with mean parameter value, thus assuming that the mean parameter value and its corresponding variance is representative of the expected range of values in a larger population. The linear model was fitted to the data points in our cohort and then scaled down to a brainstem necrosis incidence rate of 5.5% [95% confidence interval (CI): 2.9%, 10.2%] observed in a study of 179 paediatric ependymoma patients treated with proton therapy at UFHPTI between 2007 and 2017 [25], with the new slope given by the previous linear slope described relative to the incidence of 5.5%.

Logistic regression models were also constructed to evaluate the discriminative ability of the curves with respect to the cohort. The discriminative ability of the logistic regression models was compared to a random forest classifier, a neural network and a support vector machine trained on the same data. These machine learning methods were

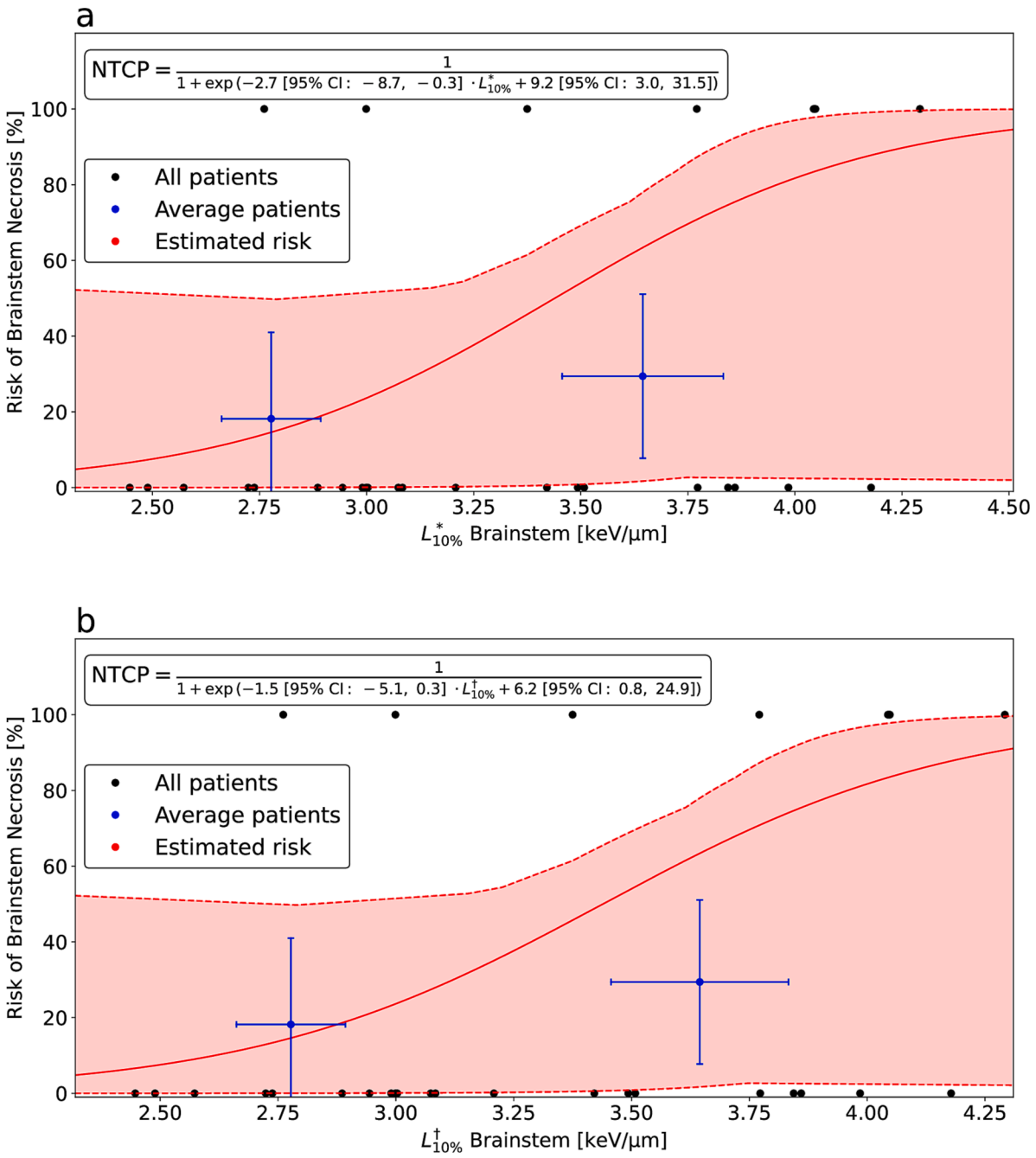

Fig. 3. Logistic regression models showing risk of brainstem necrosis for the patient cohort without a scaling factor associated with the $L_{10\%}$ ($D > 54$ Gy(RBE) marked with a * and the $L_{10\%}$ ($D > 50$ Gy(RBE) marked with a †. 95% CIs for the regression curves are shown in dashed red lines with the shaded red area describing the area covered by the CIs. Each individual patient in the case-control cohort is plotted as a black point. a) is a logistic regression model associating brainstem necrosis risk with the $L_{10\%}$ ($D > 54$ Gy(RBE) where the patient cohort is shown divided in two shown in blue based on whether they had $L_{10\%}$ ($D > 54$ Gy(RBE) over or under 3 keV/µm. b) a) is a logistic regression model associating brainstem necrosis risk with the $L_{10\%}$ ($D > 50$ Gy(RBE) where the patient cohort is shown divided in two shown in blue based on whether they had $L_{10\%}$ ($D > 54$ Gy(RBE) over or under 3.5 keV/µm. (For interpretation of the references to colour in this figure legend, the reader is referred to the web version of this article.)

generated using the sci-kit learn package in python [26]. 95% CIs for the fitted model parameters were constructed by bootstrapping samples in 10^4 iterations and fitting new models on the new samples. The top and bottom 2.5% of parameters were then excluded to give the final intervals.

2.5. Model evaluation

The models were evaluated based on the area under the receiver operating characteristic (AUC) curve, the area under the precision recall curve (AUPRC) and Brier score. Leave one out cross-validation (LOOCV) gave a measure of the models' generalisability. Here a model was established based on all data points except one, and the model then predicted the value of the excluded data point. The process was repeated for each data point and prediction accuracy was calculated. All metrics were calculated in Python using the sci-kit learn package [26].

Calibration curves were used to evaluate the calibration of the logistic regression models and in what ranges they over or underpredict toxicity risk. The curves were calculated using the sci-kit learn Python package [26].

Table 1
Area under receiver operating characteristic (AUC) curve, area under precision-recall curve (AUPRC), Brier score and leave one out cross-validated (LOOCV) accuracy of both univariate and bivariate logistic regression models.

Predictor(s)	AUC	AUPRC	Brier Score	Accuracy (LOOCV)
$L_{10\%}$* Brainstem	0.76	0.63	0.15	79%
$L^{\dagger}_{10\%}$ Brainstem	0.70	0.52	0.17	71%
$L_{10\%}$* Brainstem and Volume of Anterior Pons	0.84	0.81	0.11	89%

*Dose threshold 54 Gy(RBE), †Dose threshold 50 Gy(RBE).

2.6. Power analysis

Due to limited sample size and as a consequence low statistical power, a power analysis was performed to determine the number of patients required to establish models with greater statistical power by assuming identical data characteristics, setting 80% statistical power as a required threshold. Further details on the power analysis are provided in Supplementary material C.

3. Results

The $L_{10\%}$ of the brainstem volume receiving dose over 54 Gy(RBE) was found to be the parameter most closely related to toxicity, with a 1 keV/μm increase being associated with an increased risk [CI] of brainstem necrosis of 46 [4, 77] percentage points (Fig. 1a) based on the case-control cohort only. The CIs of the curves were wide, but the slope was positive in the whole interval. When utilising a base incidence rate from the literature, an increase in 1 keV/μm yielded an increase in absolute risk of 2.5 [0.0, 7.8] percentage points (Fig. 1b). In the $L_{10\%}$ ($D > 54$ Gy (RBE)) interval observed in this case-control cohort (2.33, 3.80 keV/μm) we found absolute risk of brainstem necrosis ranging from 4.0% [2.8%, 5.5%] to 7.7% [3.0%, 17.0%] (Fig. 1b). When the $L_{10\%}$ ($D > 50$ Gy (RBE)) was utilised instead of the $L_{10\%}$ ($D > 54$ Gy(RBE)), the risk associated with a 1 keV/μm increase changed to 1.5 [−0.1, 5.5] percentage points (Fig. 2).

The univariate logistic regression models incorporating the $L_{10\%}$ ($D > 54$ Gy(RBE)) (Fig. 3a) and the $L_{10\%}$ ($D > 50$ Gy(RBE)) (Fig. 3b) achieved discriminative ability as quantified by the performance metrics shown in Table 1. A bivariate model combining the $L_{10\%}$ ($D > 54$ Gy (RBE)) and the volume of the brainstem anterior pons (Equation D1) was also fitted and improved all performance measures from the $L_{10\%}$ ($D > 54$ Gy(RBE)) only model, with an AUC increasing from 0.76 to 0.84 and the LOOCV accuracy increasing from 79% to 89% (Table 1). The machine learning algorithms showed similar model performance compared to logistic regression, except the bivariate neural network which showed excellent performance on all metrics except LOOCV accuracy (Table A2). The $L_{10\%}$ ($D > 54$ Gy(RBE)) logistic regression model showed slightly inferior calibration compared to the $L_{10\%}$ ($D > 50$ Gy(RBE)) model (Fig. 4). The result of going from absolute to relative risk (Fig. 1a and b) was a shallower curve and noticeably the points representing the patient cohort showed that the model went from overpredicting to underpredicting toxicity in the lower range of $L_{10\%}$ ($D > 54$ Gy(RBE)) values and from underpredicting to overpredicting toxicity in the higher range of $L_{10\%}$ ($D > 54$ Gy(RBE)) values.

The required number of symptomatic brainstem necrosis patients to achieve 80% statistical power was 19 [7, 350] for the $L_{10\%}$, 36 [11, 130] for the $L_{50\%}$ and 37 [7, 690] for the $L^{3}_{0.1\text{cm}}$ with $D > 54$ Gy(RBE). For $D > 50$ Gy(RBE) the numbers increased to 67 [10, $2.0{\cdot}10^4$], 56 [9, $2.2{\cdot}10^7$] and 54 [9, $3.4{\cdot}10^4$] for the $L_{50\%}$, $L_{10\%}$ and $L^{3}_{0.1\text{cm}}$, while no dose threshold gave 65 [9, $7.8{\cdot}10^3$], 86 [12, 830] and 84 [12, $1.5{\cdot}10^3$] for the $L_{50\%}$, $L_{10\%}$ and $L^{3}_{0.1\text{cm}}$, respectively (Fig. 5).

The patients with brainstem necrosis generally presented with higher LET_d parameters to both the full brainstem volume and most brainstem substructures compared to the controls. The remaining analysed parameters are given in Supplementary material B.

4. Discussion

In this study we fitted risk prediction models of brainstem necrosis associated with LET in high dose volumes by using a matched case-control design. The predictive models combined with incidence rates from literature suggest evaluation of LET in treatment plan assessment, although brainstem necrosis incidence and risk estimates are low. The univariate logistic regression model including the $L_{10\%}$ ($D > 54$ Gy (RBE)) and the bivariate logistic regression also including the volume of the anterior pons (Fig. B1) achieved discriminative ability described by AUCs of 0.76 and 0.84, respectively. Assuming similar LET_d trends as in our study (7 symptomatic cases), we found that 19 to 84 symptomatic cases would be required to construct models achieving 80% statistical power, depending on the included LET_d parameter.

By utilising a matched case-control design we were able to discern a trend between LET_d and brainstem necrosis that otherwise likely would have been confounded by larger differences in treatment planning dose-volume variations and patient heterogeneity. There was an increasing risk of brainstem necrosis with increasing $L_{10\%}$ in the high dose region of this cohort ($D > 54$ Gy(RBE)) and the risk was also increasing within the full CI. This could potentially translate to a significant improvement if accounted for during treatment planning. A difference in absolute brainstem necrosis risk of 3.7 percentage points [0.2, 11.5] was observed between the patients with the highest and lowest $L_{10\%}$ ($D > 54$ Gy(RBE)) in the case-control cohort, demonstrating the feasibility of reducing estimated risk within clinically realistic LET_d values by including LET_d more directly in treatment planning.

Several studies have investigated the role of brainstem dose as a driver for brainstem necrosis [17,27,28] but purely dose-based analyses are unable to detect a potential role of LET and variable proton RBE in the development of brainstem necrosis. A set of conservative dose constraints to the brainstem in paediatric proton CNS treatment have been established to minimise the risk of necrosis [29]. However, during clinical treatment planning, the variable RBE is not calculated but instead mostly accounted for qualitatively, e.g. by the positioning of the distal fall-off of treatment fields outside of organs at risk [29]. With this study we aimed to establish a model as a supportive tool for clinical implementation of LET. The LET association with asymptomatic image changes in paediatric CNS patients has been investigated in several studies [12–14,16] where three of four studies found significant association between image changes and LET. Our current study and previous investigations [19] also showed trends towards increased risk of brainstem necrosis with increased LET_d values particularly in high dose volumes, further emphasising continued study of the role of combined high dose and high LET in critical organs such as the brainstem.

Wagenaar et al. recently estimated a required cohort size of 15 000 patients to definitely associate mean LET_d and dose on a voxel-wise basis to toxicity in a cohort of 100 unmatched head and neck patients [30]. The power analysis performed in assessment of our study established significantly lower cohort sizes to achieve statistical power of 80%, although the assumption that similar trends to the ones observed in this data will be observed in a larger similar cohort as well is subject to considerable uncertainty. Nevertheless, this demonstrates how statistical power can be achieved with more realistic cohort sizes by varying study design, which may be key in future evidence of LET-related clinical effects. However, it is important to mention the distinction between the NTCP endpoints studied here and by Wagenaar et al. A small volume of high dose and LET in an organ is easier to associate with an NTCP endpoint in a serial organ compared to a parallel organ where mean dose and LET are relevant and volumes of potentially increased LET may, therefore, be compensated due to averaging. For the studied ependymoma patients in risk of brainstem toxicity, the high LET parameters of the high dose region appear as central components. Dose-LET volume histograms as presented by Yang et al. [31] further demonstrate a

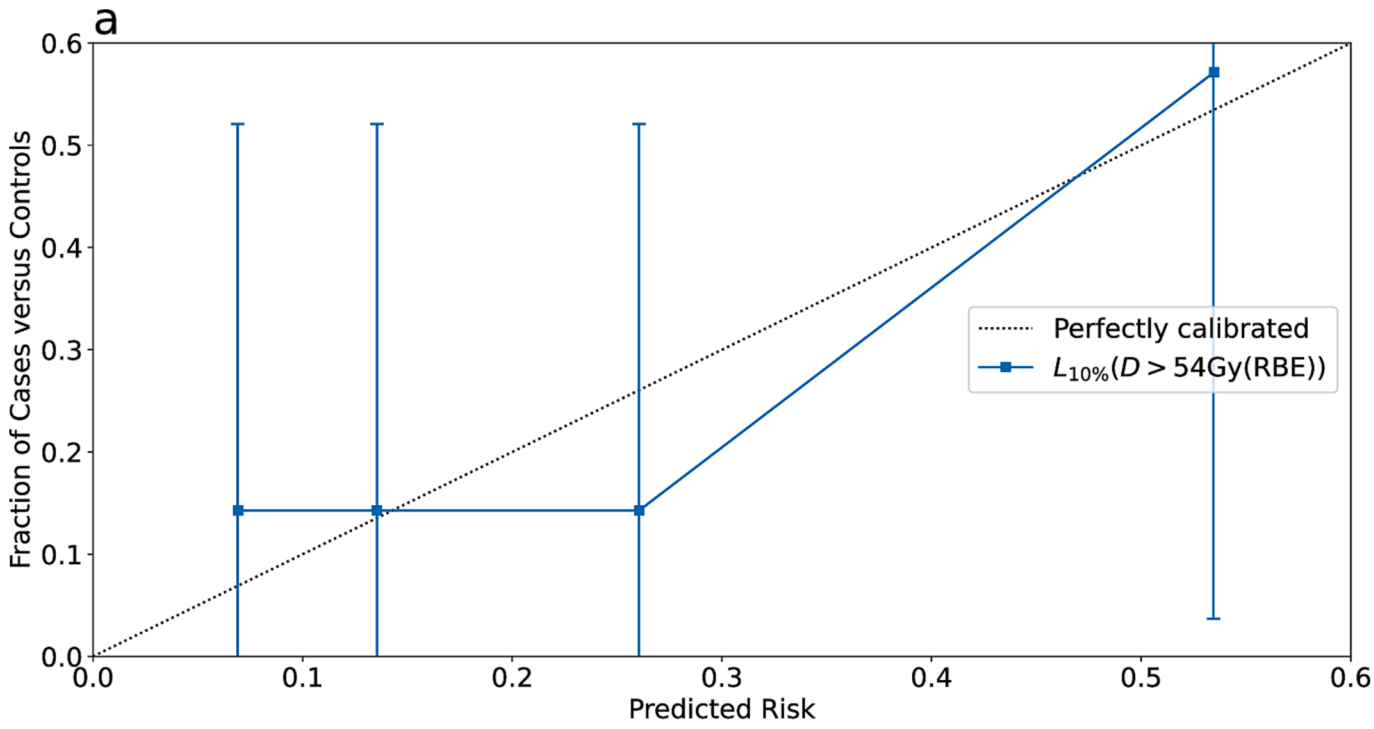

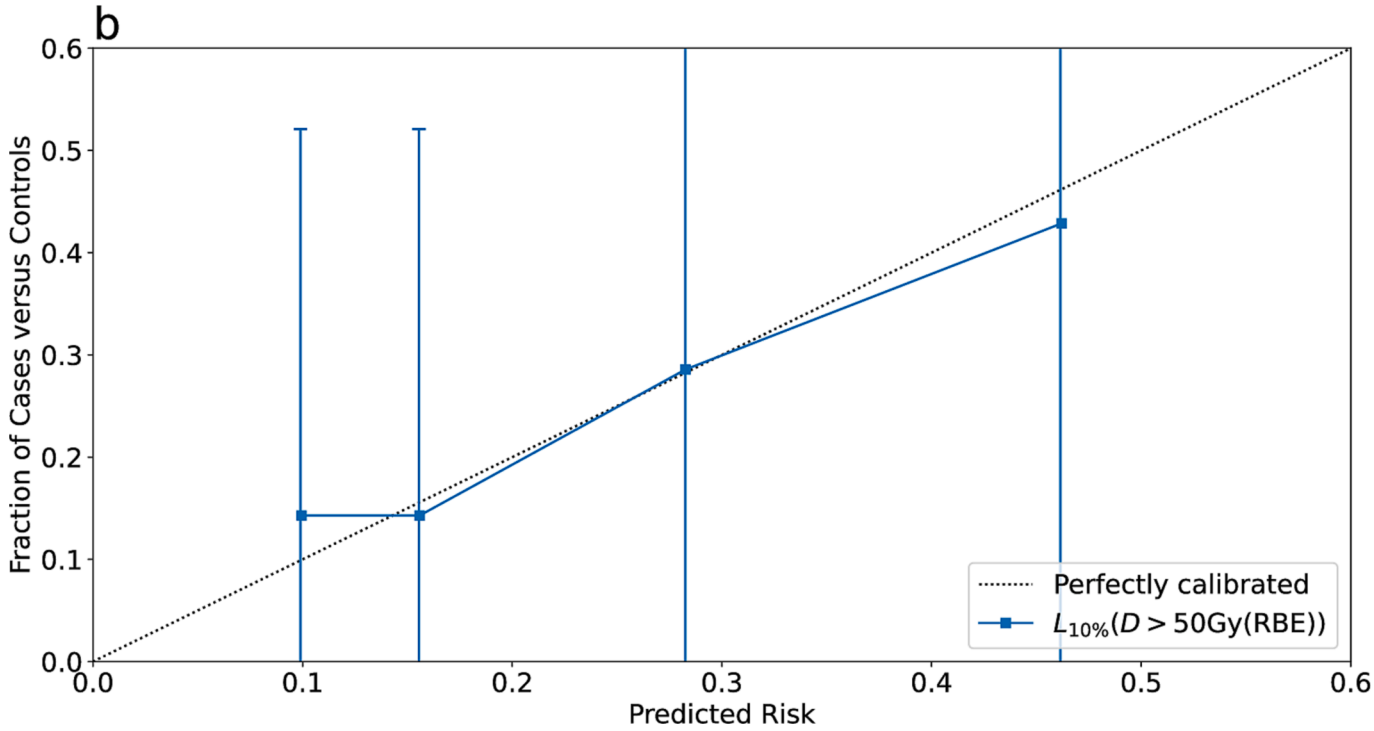

Fig. 4. Calibration curves for the logistic regression models showing deviance between the actual model and a perfectly calibrated model for the a) risk associated with the $L_{10\%}$ ($D > 54$ Gy(RBE) and the b) risk associated with the $L_{10\%}$ ($D > 50$ Gy(RBE). The patient cohort of 28 patients is divided into four groups with seven patients in each group sorted by ascending order of parameter value. The standard deviation in incidence is given by the error bars in the y-direction.

possible route of quantitative combined dose and LET assessment. Indeed, how dose and LET should be weighted relatively to each other lacks consensus. Variable RBE-models are one way to combine the parameters to describe the clinical consequence of LET, but these models are currently uncertain and largely based on *in vitro* data [32]. Yet another uncertainty aspect is the differences across reported values of LET between studies, including averaging method, particles accounted for and to what medium LET is calculated [21,33,34]. This might also affect the accuracy of the results, where LET was based on primary and secondary particles only, while the actual RBE might also be

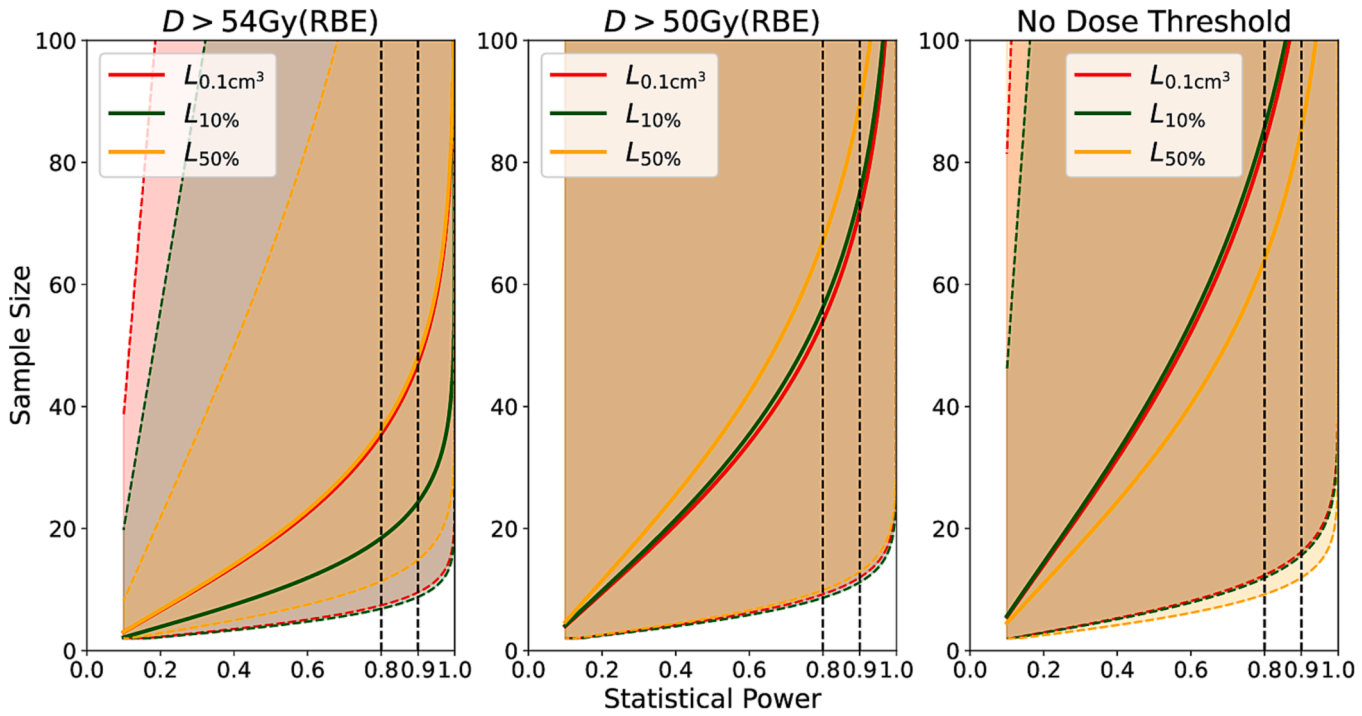

Fig. 5. Power analysis of LET_d parameters for the brainstem with a dose threshold of 54 Gy(RBE) to the left, 50 Gy(RBE) in the middle and no threshold to the right. The points of 80% and 90% statistical power are illustrated by black dotted lines. 95% CIs are shown by dotted coloured lines and the area within the CIs is shaded the corresponding colour.

significantly impacted by other particles. Further, it has also been suggested that alternative descriptions of microscopic energy deposition might more accurately describe the RBE of the proton [35]. Yet another alternative approach reported recently is to consider LET indirectly by calculating RBE based on proton track-ends instead [36].

The absolute risk of necrosis reported in this work could potentially be underestimated since the brainstem dose was generally high in our cohort. The study used for normalising the estimated risk did not report dose/volume parameters to the brainstem. However, in a larger study of 313 paediatric patients receiving dose over 50.4 Gy(RBE) to the brainstem, Indelicato et al. found a necrosis incidence of 3.8% ± 1.1% with a V54Gy(RBE) of 26% [range 0%, 100%] [17]. For comparison, our cohort had a V54Gy(RBE) of 45% [range 7%, 95%] and although the incidence rate normalised to in this work was slightly higher it might not sufficiently compensate for the increase in brainstem dose. Contrarily, in a study of 216 posterior fossa tumour patients (56 ependymomas), Gentile et al. found a brainstem necrosis rate of 1.9% (3.6% considering ependymoma only) and a V54Gy(RBE) of 44.9% [range 0%-100%] for all patients [28], thus comparing quite well with the V54Gy(RBE) of our work. However, considering all 954 patients, the brainstem necrosis rate was low at 1.7%. This might have the opposite effect and bias our models towards higher risk estimates. The normalisation was performed to address this bias and to centre the models around more established incidence rates.

In the study of rare outcomes such as brainstem necrosis, gathering sufficient data for statistical certainty is difficult. In this study we analysed a large number of parameters for a relatively small dataset which might be problematic since setting a threshold of 5% for statistical significance means we accept a one in twenty probability of tested parameters showing as statistically significant despite actually being normally distributed around origin. Considering the substructure analysis, we analysed 130 parameters, reduced to 13 if only accounting for the full brainstem volume. Thus, particularly for the substructure analysis, there is a considerable risk of false positives.

The use of the anterior pons as a secondary model parameter is not supported by literary evidence. It is therefore difficult to conclude only based on this work that there is significance with this particular substructure, especially since the substructure is the smallest sub-volume analysed and therefore the most sensitive to systematic errors in contouring.

In conclusion, NTCP models for brainstem necrosis accounting for the LET_d of protons were constructed and suggest hotspots of high LET_d in high dose volumes to be associated with the development of brainstem necrosis. We emphasise the importance of further investigating LET in the scope of toxicity and to account for LET and variable RBE both in proton therapy plan optimisation and evaluation.

Declaration of Competing Interest

The authors declare that they have no known competing financial interests or personal relationships that could have appeared to influence the work reported in this paper.

Acknowledgements

The authors wish to thank Johannes Tjelta, MSc, and Peter Magnus T. Lægdsmand, MSc, for valuable input on the contents of this paper. We would also like to thank Professor Ivan R Vogelius, PhD for discussions regarding the model design. This work was partly funded by Helse Vest RHF (grant no. F-12581), the Trond Mohn foundation (grant no. BFS2015TMT03), the Bioproton project (326218), Research council of Norway, the Norwegian Cancer Society (202089) and the Norwegian Childhood Cancer Society (210007).

Appendix A. Supplementary data

Supplementary data to this article can be found online at https://doi.org/10.1016/j.phro.2023.100466.

References

[1] Reni M, Gatta G, Mazza E, Vecht C. Ependymoma. Crit Rev Oncol Hematol 2007; 63:81–9. https://doi.org/10.1016/j.critrevonc.2007.03.004.

[2] Indelicato DJ, Ioakeim-Ioannidou M, Bradley JA, Mailhot-Vega RB, Morris CG, Tarbell NJ, et al. Proton therapy for pediatric ependymoma: mature results from a bicentric study. Int J Radiat Oncol Biol Phys 2021;110:815–20. https://doi.org/10.1016/j.ijrobp.2021.01.027.

[3] Upadhyay R, Liao K, Grosshans DR, McGovern SL, McAleer MF, Zaky W, et al. Quantifying the risk and dosimetric variables of symptomatic brainstem injury after proton beam radiation in pediatric brain tumors. Neuro Oncol 2022;24: 1571–81. https://doi.org/10.1093/neuonc/noac044.

[4] Constine LS, Ronckers CM, Hua CH, Olch A, Kremer LCM, Jackson A, et al. Pediatric normal tissue effects in the clinic (PENTEC): an international collaboration to analyse normal tissue radiation dose-volume response relationships for paediatric cancer patients. Clin Oncol (R Coll Radiol) 2019;31: 199–207. https://doi.org/10.1016/j.clon.2019.01.002.

[5] Paganetti H. Relating proton treatments to photon treatments via the relative biological effectiveness-should we revise current clinical practice? Int J Radiat Oncol Biol Phys 2015;91:892–4. https://doi.org/10.1016/j.ijrobp.2014.11.021.

[6] Paganetti H. Relative biological effectiveness (RBE) values for proton beam therapy. Variations as a function of biological endpoint, dose, and linear energy transfer. Phys Med Biol 2014;59:R419–72. https://doi.org/10.1088/0031-9155/59/22/R419.

[7] Underwood TSA, McNamara AL, Appelt A, Haviland JS, Sørensen BS, Troost EGC. A systematic review of clinical studies on variable proton relative biological effectiveness (RBE). Radiother Oncol 2022;175:79–92. https://doi.org/10.1016/j.radonc.2022.08.014.

[8] Paganetti H. Mechanisms and review of clinical evidence of variations in relative biological effectiveness in proton therapy. Int J Radiat Oncol Biol Phys 2022;112: 222–36. https://doi.org/10.1016/j.ijrobp.2021.08.015.

[9] Bertolet A, Abolfath R, Carlson DJ, Lustig RA, Hill-Kayser C, Alonso-Basanta M, et al. Correlation of LET With MRI changes in brain and potential implications for normal tissue complication probability for patients with meningioma treated with pencil beam scanning proton therapy. Int J Radiat Oncol Biol Phys 2022;112: 237–46. https://doi.org/10.1016/j.ijrobp.2021.08.027.

[10] Engeseth GM, He R, Mirkovic D, Yepes P, Mohamed ASR, Stieb S, et al. Mixed effect modeling of dose and linear energy transfer correlations with brain image changes after intensity modulated proton therapy for skull base head and neck cancer. Int J Radiat Oncol Biol Phys 2021;111:684–92. https://doi.org/10.1016/j.ijrobp.2021.06.016.

[11] Niemierko A, Schuemann J, Niyazi M, Giantsoudi D, Maquilan G, Shih HA, et al. Brain necrosis in adult patients after proton therapy: is there evidence for dependency on linear energy transfer? Int J Radiat Oncol Biol Phys 2021;109: 109–19. https://doi.org/10.1016/j.ijrobp.2020.08.058.

[12] Bolsi A, Placidi L, Pica A, Ahlhelm FJ, Walser M, Lomax AJ, et al. Pencil beam scanning proton therapy for the treatment of craniopharyngioma complicated with radiation-induced cerebral vasculopathies: a dosimetric and linear energy transfer (LET) evaluation. Radiother Oncol 2020;149:197–204. https://doi.org/10.1016/j.radonc.2020.04.052.

[13] Bahn E, Bauer J, Harrabi S, Herfarth K, Debus J, Alber M. Late contrast enhancing brain lesions in proton-treated patients with low-grade glioma: clinical evidence for increased periventricular sensitivity and variable RBE. Int J Radiat Oncol Biol Phys 2020;107:571–8. https://doi.org/10.1016/j.ijrobp.2020.03.013.

[14] Ödén J, Toma-Dasu I, Witt Nyström P, Traneus E, Dasu A. Spatial correlation of linear energy transfer and relative biological effectiveness with suspected treatment-related toxicities following proton therapy for intracranial tumors. Med Phys 2020;47:342–51. https://doi.org/10.1002/mp.13911.

[15] Eulitz J, Troost EGC, Raschke F, Schulz E, Lutz B, Dutz A, et al. Predicting late magnetic resonance image changes in glioma patients after proton therapy. Acta Oncol 2019;58:1536–9. https://doi.org/10.1080/0284186X.2019.1631477.

[16] Peeler CR, Mirkovic D, Titt U, Blanchard P, Gunther JR, Mahajan A, et al. Clinical evidence of variable proton biological effectiveness in pediatric patients treated for ependymoma. Radiother Oncol 2016;121:395–401. https://doi.org/10.1016/j.radonc.2016.11.001.

[17] Indelicato DJ, Flampouri S, Rotondo RL, Bradley JA, Morris CG, Aldana PR, et al. Incidence and dosimetric parameters of pediatric brainstem toxicity following proton therapy. Acta Oncol 2014;53:1298–304. https://doi.org/10.3109/0284186X.2014.957414.

[18] J. Eulitz G. C. Troost E, Klünder L, Raschke F, Hahn C, Schulz E, et al. Increased relative biological effectiveness and periventricular radiosensitivity in proton therapy of glioma patients Radiother Oncol 178 2023 109422 https://doi.org/ https://doi.org/10.1016/j.radonc.2022.11.011.

[19] Fjæra LF, Indelicato DJ, Handeland AH, Ytre-Hauge KS, Lassen-Ramshad Y, Muren LP, et al. A case-control study of linear energy transfer and relative biological effectiveness related to symptomatic brainstem toxicity following pediatric proton therapy. Radiother Oncol 2022;175:47–55. https://doi.org/10.1016/j.radonc.2022.07.022.

[20] Gaito S, Burnet N, Aznar M, Crellin A, Indelicato DJ, Ingram S, et al. Normal tissue complication probability modelling for toxicity prediction and patient selection in proton beam therapy to the central nervous system: a literature review. e225–e237 Clin Oncol (R Coll Radiol) 2022;34. https://doi.org/10.1016/j.clon.2021.12.015.

[21] Engeseth GM, Stokkevåg C, Muren LP. Achievements and challenges in normal tissue response modelling for proton therapy. Phys Imaging Radiat Oncol 2022;24: 118–20. https://doi.org/10.1016/j.phro.2022.11.004.

[22] Pearce N. Analysis of matched case-control studies. BMJ 2016;352:i969. https://doi.org/10.1136/bmj.i969.

[23] Fjæra LF, Indelicato DJ, Stokkevåg CH, Muren LP, Hsi WC, Ytre-Hauge KS. Implementation of a double scattering nozzle for Monte Carlo recalculation of proton plans with variable relative biological effectiveness. Phys Med Biol 2020; 65:225033. https://doi.org/10.1088/1361-6560/abc12d.

[24] Darby SC, Ewertz M, McGale P, Bennet AM, Blom-Goldman U, Brønnum D, et al. Risk of ischemic heart disease in women after radiotherapy for breast cancer. New Eng J Med 2013;368:987–98. https://doi.org/10.1056/NEJMoa1209825.

[25] Indelicato DJ, Bradley JA, Rotondo RL, Nanda RH, Logie N, Sandler ES, et al. Outcomes following proton therapy for pediatric ependymoma. Acta Oncol 2018; 57:644–8. https://doi.org/10.1080/0284186X.2017.1413248.

[26] Pedregosa F, Varoquaux G, Gramfort A, Michel V, Thirion B, Grisel O, et al. Scikit-learn: machine learning in python. J Mach Learn Res 2011;12:2825–30. https://doi.org/10.48550/arXiv.1201.0490.

[27] Vogel J, Grewal A, O'Reilly S, Lustig R, Kurtz G, Minturn JE, et al. Risk of brainstem necrosis in pediatric patients with central nervous system malignancies after pencil beam scanning proton therapy. Acta Oncol 2019;58:1752–6. https://doi.org/10.1080/0284186X.2019.1659996.

[28] Gentile MS, Yeap BY, Paganetti H, Goebel CP, Gaudet DE, Gallotto SL, et al. Brainstem injury in pediatric patients with posterior fossa tumors treated with proton beam therapy and associated dosimetric factors. Int J Radiat Oncol Biol Phys 2018;100:719–29. https://doi.org/10.1016/j.ijrobp.2017.11.026.

[29] Haas-Kogan D, Indelicato D, Paganetti H, Esiashvili N, Mahajan A, Yock T, et al. National cancer institute workshop on proton therapy for children: considerations regarding brainstem injury. Int J Radiat Oncol Biol Phys 2018;101:152–68. https://doi.org/10.1016/j.ijrobp.2018.01.013.

[30] Wagenaar D, Schuit E, van der Schaaf A, Langendijk JA, Both S. Can the mean linear energy transfer of organs be directly related to patient toxicities for current head and neck cancer intensity-modulated proton therapy practice? Radiother Oncol 2021;165:159–65. https://doi.org/10.1016/j.radonc.2021.09.003.

[31] Yang Y, Vargas CE, Bhangoo RS, Wong WW, Schild SE, Daniels TB, et al. Exploratory investigation of dose-linear energy transfer (LET) volume histogram (DLVH) for adverse events study in intensity modulated proton therapy (IMPT). Int J Radiat Oncol Biol Phys 2021;110:1189–99. https://doi.org/10.1016/j.ijrobp.2021.02.024.

[32] Rørvik E, Fjæra LF, Dahle TJ, Dale JE, Engeseth GM, Stokkevåg CH, et al. Exploration and application of phenomenological RBE models for proton therapy. Phys Med Biol 2018;63:185013. https://doi.org/10.1088/1361-6560/aad9db.

[33] Kalholm F, Grzanka L, Traneus E, Bassler N. A systematic review on the usage of averaged LET in radiation biology for particle therapy. Radiother Oncol 2021;161: 211–21. https://doi.org/10.1016/j.radonc.2021.04.007.

[34] Hahn C, Ödén J, Dasu A, Vestergaard A, Fuglsang Jensen M, Sokol O, et al. Towards harmonizing clinical linear energy transfer (LET) reporting in proton radiotherapy: a European multi-centric study. Acta Oncol 2022;61:206–14. https://doi.org/10.1080/0284186X.2021.1992007.

[35] Kalholm F, Grzanka L, Toma-Dasu I, Bassler N. Modeling RBE with other quantities than LET significantly improves prediction of in vitro cell survival for proton therapy. Med Phys 2023;50:651–9. https://doi.org/10.1002/mp.16029.

[36] Henthorn NT, Gardner LL, Aitkenhead AH, Rowland BC, Shin J, Smith EAK, et al. Proposing a clinical model for RBE based on proton track-end counts. Int J Radiat Oncol Biol Phys 2023. https://doi.org/10.1016/j.ijrobp.2022.12.056. in press.